

Measurement of the branching fractions of the radiative leptonic τ decays $\tau \rightarrow e\gamma\nu\bar{\nu}$ and $\tau \rightarrow \mu\gamma\nu\bar{\nu}$ at *BABAR*

J. P. Lees,¹ V. Poireau,¹ V. Tisserand,¹ E. Grauges,² A. Palano^{ab,3} G. Eigen,⁴ B. Stugu,⁴ D. N. Brown,⁵ L. T. Kerth,⁵ Yu. G. Kolomensky,⁵ M. J. Lee,⁵ G. Lynch,⁵ H. Koch,⁶ T. Schroeder,⁶ C. Hearty,⁷ T. S. Mattison,⁷ J. A. McKenna,⁷ R. Y. So,⁷ A. Khan,⁸ V. E. Blinov^{abc,9} A. R. Buzykaev^{a,9} V. P. Druzhinin^{ab,9} V. B. Golubev^{ab,9} E. A. Kravchenko^{ab,9} A. P. Onuchin^{abc,9} S. I. Serednyakov^{ab,9} Yu. I. Skovpen^{ab,9} E. P. Solodov^{ab,9} K. Yu. Todyshev^{ab,9} A. J. Lankford,¹⁰ B. Dey,¹¹ J. W. Gary,¹¹ O. Long,¹¹ M. Franco Sevilla,¹² T. M. Hong,¹² D. Kovalskiy,¹² J. D. Richman,¹² C. A. West,¹² A. M. Eisner,¹³ W. S. Lockman,¹³ W. Panduro Vazquez,¹³ B. A. Schumm,¹³ A. Seiden,¹³ D. S. Chao,¹⁴ C. H. Cheng,¹⁴ B. Echenard,¹⁴ K. T. Flood,¹⁴ D. G. Hitlin,¹⁴ T. S. Miyashita,¹⁴ P. Ongmongkolkul,¹⁴ F. C. Porter,¹⁴ M. Röhrken,¹⁴ R. Andreassen,¹⁵ Z. Huard,¹⁵ B. T. Meadows,¹⁵ B. G. Pushpawela,¹⁵ M. D. Sokoloff,¹⁵ L. Sun,¹⁵ P. C. Bloom,¹⁶ W. T. Ford,¹⁶ A. Gaz,¹⁶ J. G. Smith,¹⁶ S. R. Wagner,¹⁶ R. Ayad,^{17,*} W. H. Toki,¹⁷ B. Spaan,¹⁸ D. Bernard,¹⁹ M. Verderi,¹⁹ S. Playfer,²⁰ D. Bettoni^{a,21} C. Bozzi^{a,21} R. Calabrese^{ab,21} G. Cibinetto^{ab,21} E. Fioravanti^{ab,21} I. Garzia^{ab,21} E. Luppi^{ab,21} L. Piemontese^{a,21} V. Santoro^{a,21} A. Calcaterra,²² R. de Sangro,²² G. Finocchiaro,²² S. Martellotti,²² P. Patteri,²² I. M. Peruzzi,^{22,†} M. Piccolo,²² M. Rama,²² A. Zallo,²² R. Contri^{ab,23} M. R. Monge^{ab,23} S. Passaggio^{a,23} C. Patrignani^{ab,23} B. Bhuyan,²⁴ V. Prasad,²⁴ A. Adametz,²⁵ U. Uwer,²⁵ H. M. Lacker,²⁶ U. Mallik,²⁷ C. Chen,²⁸ J. Cochran,²⁸ S. Prell,²⁸ H. Ahmed,²⁹ A. V. Gritsan,³⁰ N. Arnaud,³¹ M. Davier,³¹ D. Derkach,³¹ G. Grosdidier,³¹ F. Le Diberder,³¹ A. M. Lutz,³¹ B. Malaescu,^{31,‡} P. Roudeau,³¹ A. Stocchi,³¹ G. Wormser,³¹ D. J. Lange,³² D. M. Wright,³² J. P. Coleman,³³ J. R. Fry,³³ E. Gabathuler,³³ D. E. Hutchcroft,³³ D. J. Payne,³³ C. Touramanis,³³ A. J. Bevan,³⁴ F. Di Lodovico,³⁴ R. Sacco,³⁴ G. Cowan,³⁵ D. N. Brown,³⁶ C. L. Davis,³⁶ A. G. Denig,³⁷ M. Fritsch,³⁷ W. Gradl,³⁷ K. Griessinger,³⁷ A. Hafner,³⁷ K. R. Schubert,³⁷ R. J. Barlow,^{38,§} G. D. Lafferty,³⁸ R. Cenci,³⁹ B. Hamilton,³⁹ A. Jawahery,³⁹ D. A. Roberts,³⁹ R. Cowan,⁴⁰ R. Cheaib,⁴¹ P. M. Patel,^{41,¶} S. H. Robertson,⁴¹ N. Neria^{a,42} F. Palombo^{ab,42} L. Cremaldi,⁴³ R. Godang,^{43,**} D. J. Summers,⁴³ M. Simard,⁴⁴ P. Taras,⁴⁴ G. De Nardo^{ab,45} G. Onorato^{ab,45} C. Sciacca^{ab,45} G. Raven,⁴⁶ C. P. Jessop,⁴⁷ J. M. LoSecco,⁴⁷ K. Honscheid,⁴⁸ R. Kass,⁴⁸ M. Margoni^{ab,49} M. Morandin^{a,49} M. Posocco^{a,49} M. Rotondo^{a,49} G. Simi^{ab,49} F. Simonetto^{ab,49} R. Stroili^{ab,49} S. Akar,⁵⁰ E. Ben-Haim,⁵⁰ M. Bomben,⁵⁰ G. R. Bonneaud,⁵⁰ H. Briand,⁵⁰ G. Calderini,⁵⁰ J. Chauveau,⁵⁰ Ph. Leruste,⁵⁰ G. Marchiori,⁵⁰ J. Ocariz,⁵⁰ M. Biasini^{ab,51} E. Manoni^{a,51} A. Rossi^{a,51} C. Angelini^{ab,52} G. Batignani^{ab,52} S. Bettarini^{ab,52} M. Carpinelli^{ab,52,††} G. Casarosa^{ab,52} M. Chrzaszcz^{a,52} F. Forti^{ab,52} M. A. Giorgi^{ab,52} A. Lusiani^{ac,52} B. Oberhof^{ab,52} E. Paoloni^{ab,52} G. Rizzo^{ab,52} J. J. Walsh^{a,52} D. Lopes Pegna,⁵³ J. Olsen,⁵³ A. J. S. Smith,⁵³ F. Anulli^{a,54} R. Faccini^{ab,54} F. Ferrarotto^{a,54} F. Ferroni^{ab,54} M. Gaspero^{ab,54} A. Pilloni^{ab,54} G. Piredda^{a,54} C. Bünger,⁵⁵ S. Dittrich,⁵⁵ O. Grünberg,⁵⁵ M. Hess,⁵⁵ T. Leddig,⁵⁵ C. Voß,⁵⁵ R. Waldi,⁵⁵ T. Adye,⁵⁶ E. O. Olaiya,⁵⁶ F. F. Wilson,⁵⁶ S. Emery,⁵⁷ G. Vasseur,⁵⁷ D. Aston,⁵⁸ D. J. Bard,⁵⁸ C. Cartaro,⁵⁸ M. R. Convery,⁵⁸ J. Dorfan,⁵⁸ G. P. Dubois-Felsmann,⁵⁸ W. Dunwoodie,⁵⁸ M. Ebert,⁵⁸ R. C. Field,⁵⁸ B. G. Fulson,⁵⁸ M. T. Graham,⁵⁸ C. Hast,⁵⁸ W. R. Innes,⁵⁸ P. Kim,⁵⁸ D. W. G. S. Leith,⁵⁸ D. Lindemann,⁵⁸ S. Luitz,⁵⁸ V. Luth,⁵⁸ H. L. Lynch,⁵⁸ D. B. MacFarlane,⁵⁸ D. R. Muller,⁵⁸ H. Neal,⁵⁸ M. Perl,^{58,¶¶} T. Pulliam,⁵⁸ B. N. Ratcliff,⁵⁸ A. Roodman,⁵⁸ R. H. Schindler,⁵⁸ A. Snyder,⁵⁸ D. Su,⁵⁸ M. K. Sullivan,⁵⁸ J. Va'vra,⁵⁸ W. J. Wisniewski,⁵⁸ H. W. Wulsin,⁵⁸ M. V. Purohit,⁵⁹ J. R. Wilson,⁵⁹ A. Randle-Conde,⁶⁰ S. J. Sekula,⁶⁰ M. Bellis,⁶¹ P. R. Burchat,⁶¹ E. M. T. Puccio,⁶¹ M. S. Alam,⁶² J. A. Ernst,⁶² R. Gorodeisky,⁶³ N. Guttman,⁶³ D. R. Peimer,⁶³ A. Soffer,⁶³ S. M. Spanier,⁶⁴ J. L. Ritchie,⁶⁵ R. F. Schwitters,⁶⁵ J. M. Izen,⁶⁶ X. C. Lou,⁶⁶ F. Bianchi^{ab,67} F. De Mori^{ab,67} A. Filippi^{a,67} D. Gamba^{ab,67} L. Lanceri^{ab,68} L. Vitale^{ab,68} F. Martinez-Vidal,⁶⁹ A. Oyanguren,⁶⁹ P. Villanueva-Perez,⁶⁹ J. Albert,⁷⁰ Sw. Banerjee,⁷⁰ A. Beaulieu,⁷⁰ F. U. Bernlochner,⁷⁰ H. H. F. Choi,⁷⁰ G. J. King,⁷⁰ R. Kowalewski,⁷⁰ M. J. Lewczuk,⁷⁰ T. Lueck,⁷⁰ I. M. Nugent,⁷⁰ J. M. Roney,⁷⁰ R. J. Sobie,⁷⁰ N. Tasneem,⁷⁰ T. J. Gershon,⁷¹ P. F. Harrison,⁷¹ T. E. Latham,⁷¹ H. R. Band,⁷² S. Dasu,⁷² Y. Pan,⁷² R. Prepost,⁷² and S. L. Wu⁷²

(The *BABAR* Collaboration)

¹Laboratoire d'Annecy-le-Vieux de Physique des Particules (LAPP),
Université de Savoie, CNRS/IN2P3, F-74941 Annecy-Le-Vieux, France

²Universitat de Barcelona, Facultat de Física, Departament ECM, E-08028 Barcelona, Spain

³INFN Sezione di Bari^a; Dipartimento di Fisica, Università di Bari^b, I-70126 Bari, Italy

⁴University of Bergen, Institute of Physics, N-5007 Bergen, Norway

- ⁵Lawrence Berkeley National Laboratory and University of California, Berkeley, California 94720, USA
- ⁶Ruhr Universität Bochum, Institut für Experimentalphysik 1, D-44780 Bochum, Germany
- ⁷University of British Columbia, Vancouver, British Columbia, Canada V6T 1Z1
- ⁸Brunel University, Uxbridge, Middlesex UB8 3PH, United Kingdom
- ⁹Budker Institute of Nuclear Physics SB RAS, Novosibirsk 630090^a,
Novosibirsk State University, Novosibirsk 630090^b,
Novosibirsk State Technical University, Novosibirsk 630092^c, Russia
- ¹⁰University of California at Irvine, Irvine, California 92697, USA
- ¹¹University of California at Riverside, Riverside, California 92521, USA
- ¹²University of California at Santa Barbara, Santa Barbara, California 93106, USA
- ¹³University of California at Santa Cruz, Institute for Particle Physics, Santa Cruz, California 95064, USA
- ¹⁴California Institute of Technology, Pasadena, California 91125, USA
- ¹⁵University of Cincinnati, Cincinnati, Ohio 45221, USA
- ¹⁶University of Colorado, Boulder, Colorado 80309, USA
- ¹⁷Colorado State University, Fort Collins, Colorado 80523, USA
- ¹⁸Technische Universität Dortmund, Fakultät Physik, D-44221 Dortmund, Germany
- ¹⁹Laboratoire Leprince-Ringuet, Ecole Polytechnique, CNRS/IN2P3, F-91128 Palaiseau, France
- ²⁰University of Edinburgh, Edinburgh EH9 3JZ, United Kingdom
- ²¹INFN Sezione di Ferrara^a; Dipartimento di Fisica e Scienze della Terra, Università di Ferrara^b, I-44122 Ferrara, Italy
- ²²INFN Laboratori Nazionali di Frascati, I-00044 Frascati, Italy
- ²³INFN Sezione di Genova^a; Dipartimento di Fisica, Università di Genova^b, I-16146 Genova, Italy
- ²⁴Indian Institute of Technology Guwahati, Guwahati, Assam, 781 039, India
- ²⁵Universität Heidelberg, Physikalisches Institut, D-69120 Heidelberg, Germany
- ²⁶Humboldt-Universität zu Berlin, Institut für Physik, D-12489 Berlin, Germany
- ²⁷University of Iowa, Iowa City, Iowa 52242, USA
- ²⁸Iowa State University, Ames, Iowa 50011-3160, USA
- ²⁹Physics Department, Jazan University, Jazan 22822, Kingdom of Saudi Arabia
- ³⁰Johns Hopkins University, Baltimore, Maryland 21218, USA
- ³¹Laboratoire de l'Accélérateur Linéaire, IN2P3/CNRS et Université Paris-Sud 11,
Centre Scientifique d'Orsay, F-91898 Orsay Cedex, France
- ³²Lawrence Livermore National Laboratory, Livermore, California 94550, USA
- ³³University of Liverpool, Liverpool L69 7ZE, United Kingdom
- ³⁴Queen Mary, University of London, London, E1 4NS, United Kingdom
- ³⁵University of London, Royal Holloway and Bedford New College, Egham, Surrey TW20 0EX, United Kingdom
- ³⁶University of Louisville, Louisville, Kentucky 40292, USA
- ³⁷Johannes Gutenberg-Universität Mainz, Institut für Kernphysik, D-55099 Mainz, Germany
- ³⁸University of Manchester, Manchester M13 9PL, United Kingdom
- ³⁹University of Maryland, College Park, Maryland 20742, USA
- ⁴⁰Massachusetts Institute of Technology, Laboratory for Nuclear Science, Cambridge, Massachusetts 02139, USA
- ⁴¹McGill University, Montréal, Québec, Canada H3A 2T8
- ⁴²INFN Sezione di Milano^a; Dipartimento di Fisica, Università di Milano^b, I-20133 Milano, Italy
- ⁴³University of Mississippi, University, Mississippi 38677, USA
- ⁴⁴Université de Montréal, Physique des Particules, Montréal, Québec, Canada H3C 3J7
- ⁴⁵INFN Sezione di Napoli^a; Dipartimento di Scienze Fisiche,
Università di Napoli Federico II^b, I-80126 Napoli, Italy
- ⁴⁶NIKHEF, National Institute for Nuclear Physics and High Energy Physics, NL-1009 DB Amsterdam, The Netherlands
- ⁴⁷University of Notre Dame, Notre Dame, Indiana 46556, USA
- ⁴⁸Ohio State University, Columbus, Ohio 43210, USA
- ⁴⁹INFN Sezione di Padova^a; Dipartimento di Fisica, Università di Padova^b, I-35131 Padova, Italy
- ⁵⁰Laboratoire de Physique Nucléaire et de Hautes Energies,
IN2P3/CNRS, Université Pierre et Marie Curie-Paris6,
Université Denis Diderot-Paris7, F-75252 Paris, France
- ⁵¹INFN Sezione di Perugia^a; Dipartimento di Fisica, Università di Perugia^b, I-06123 Perugia, Italy
- ⁵²INFN Sezione di Pisa^a; Dipartimento di Fisica,
Università di Pisa^b; Scuola Normale Superiore di Pisa^c, I-56127 Pisa, Italy
- ⁵³Princeton University, Princeton, New Jersey 08544, USA
- ⁵⁴INFN Sezione di Roma^a; Dipartimento di Fisica,
Università di Roma La Sapienza^b, I-00185 Roma, Italy
- ⁵⁵Universität Rostock, D-18051 Rostock, Germany
- ⁵⁶Rutherford Appleton Laboratory, Chilton, Didcot, Oxon, OX11 0QX, United Kingdom
- ⁵⁷CEA, Irfu, SPP, Centre de Saclay, F-91191 Gif-sur-Yvette, France
- ⁵⁸SLAC National Accelerator Laboratory, Stanford, California 94309 USA
- ⁵⁹University of South Carolina, Columbia, South Carolina 29208, USA
- ⁶⁰Southern Methodist University, Dallas, Texas 75275, USA

⁶¹Stanford University, Stanford, California 94305-4060, USA

⁶²State University of New York, Albany, New York 12222, USA

⁶³Tel Aviv University, School of Physics and Astronomy, Tel Aviv, 69978, Israel

⁶⁴University of Tennessee, Knoxville, Tennessee 37996, USA

⁶⁵University of Texas at Austin, Austin, Texas 78712, USA

⁶⁶University of Texas at Dallas, Richardson, Texas 75083, USA

⁶⁷INFN Sezione di Torino^a; Dipartimento di Fisica, Università di Torino^b, I-10125 Torino, Italy

⁶⁸INFN Sezione di Trieste^a; Dipartimento di Fisica, Università di Trieste^b, I-34127 Trieste, Italy

⁶⁹IFIC, Universitat de Valencia-CSIC, E-46071 Valencia, Spain

⁷⁰University of Victoria, Victoria, British Columbia, Canada V8W 3P6

⁷¹Department of Physics, University of Warwick, Coventry CV4 7AL, United Kingdom

⁷²University of Wisconsin, Madison, Wisconsin 53706, USA

We perform a measurement of the $\tau \rightarrow l\gamma\nu\bar{\nu}$ ($l = e, \mu$) branching fractions for a minimum photon energy of 10 MeV in the τ rest frame, using 431 fb⁻¹ of e^+e^- collisions collected at the center-of-mass energy of the $\Upsilon(4S)$ resonance with the BABAR detector at the PEP-II storage rings. We find $\mathcal{B}(\tau \rightarrow \mu\gamma\nu\bar{\nu}) = (3.69 \pm 0.03 \pm 0.10) \times 10^{-3}$, and $\mathcal{B}(\tau \rightarrow e\gamma\nu\bar{\nu}) = (1.847 \pm 0.015 \pm 0.052) \times 10^{-2}$, where the first quoted error is statistical, and the second is systematic. These results are substantially more precise than previous measurements.

PACS numbers: 13.30.Ce, 13.35-r, 13.40.Em, 13.40.Ks, 14.60.Fg

Leptonic τ decays are generally well suited to investigate the Lorentz structure of electroweak interactions in a model-independent way [1]. In particular, leptonic radiative decays $\tau \rightarrow l\gamma\nu\bar{\nu}$, where the charged lepton (l) is either an electron (e) or a muon (μ), have been studied for a long time because they are sensitive to the anomalous magnetic moment of the τ lepton [2]. At tree level, these decays can proceed through three Feynman diagrams depending on whether the photon is emitted by the incoming τ , the outgoing charged lepton, or the intermediate W boson, as shown in Fig. 1. The amplitude for the emission of the photon by the intermediate boson is suppressed by a factor $(m_\tau/M_W)^2$ with respect to a photon from the incoming/outgoing fermions and is thus negligible with respect to next-to-leading order (NLO) QED radiative corrections [3]. Both branching fractions have been measured by the CLEO collaboration. CLEO obtained $\mathcal{B}(\tau \rightarrow \mu\gamma\nu\bar{\nu}) = (3.61 \pm 0.16 \pm 0.35) \times 10^{-3}$, and $\mathcal{B}(\tau \rightarrow e\gamma\nu\bar{\nu}) = (1.75 \pm 0.06 \pm 0.17) \times 10^{-2}$ for a minimum photon energy of 10 MeV in the τ rest frame [4]. In addition, the OPAL collaboration finds $\mathcal{B}(\tau \rightarrow \mu\gamma\nu\bar{\nu}) = (3.0 \pm 0.4 \pm 0.5) \times 10^{-3}$ for a minimum photon energy of 20 MeV in the τ rest frame [5].

In the present work we perform a measurement of $\tau \rightarrow l\gamma\nu\bar{\nu}$ branching fractions for a minimum photon energy of 10 MeV in the τ rest frame. This analysis uses data recorded by the BABAR detector at the PEP-II asymmetric-energy e^+e^- storage rings operated at the SLAC National Accelerator Laboratory. The data sample consists of 431 fb⁻¹ of e^+e^- collisions recorded at the center-of-mass energy (CM) $\sqrt{s} = 10.58$ GeV [6]. The cross section for τ -pair production is $\sigma_{\tau\tau} = 0.919 \pm 0.003$ nb [7] corresponding to a data sample of about 400×10^6 τ -pairs. A detailed description of the BABAR detector is given elsewhere [8, 9]. Charged particle momenta are measured with a five-layer double-sided silicon vertex tracker and a 40-layer helium-isobutane drift chamber inside a 1.5 T superconducting solenoid magnet. An electromagnetic calorimeter (EMC) consisting of 6580 CsI(Tl) crystals is used to measure electron and photon energies; a ring-imaging Cherenkov detector is used to identify charged hadrons; the instrumented magnetic flux return (IFR) is used for muon identification. About half of the data were taken with the IFR embedded with resistive plate chambers, later partially replaced by limited streamer tubes.

For this analysis, a Monte Carlo (MC) simulation is used to estimate the signal efficiency and to optimize the selection algorithm. Simulated τ -pair events are generated using KK2f [10] and τ decays are simulated with Tauola [11]. Final-state radiative effects for τ decays in Tauola are simulated using Photos [12]. A signal τ -pair MC sample is generated where one of the τ leptons decays to $\tau \rightarrow l\gamma\nu\bar{\nu}$, and the other decays according to known decay modes [13]. For the signal sample we require the minimum photon energy in the τ rest frame to be $E_{\gamma,\min}^* > 10$ MeV. The $\tau \rightarrow l\gamma\nu\bar{\nu}$ decays with $E_{\gamma,\min}^* < 10$ MeV are treated as background. A separate τ -pair MC sample is generated requiring each τ lepton to decay in a mode based on current experimental knowledge; we exclude signal events in the former sample to

*Now at: University of Tabuk, Tabuk 71491, Saudi Arabia

†Also at: Università di Perugia, Dipartimento di Fisica, I-06123 Perugia, Italy

‡Now at: Laboratoire de Physique Nucléaire et de Hautes Energies, IN2P3/CNRS, F-75252 Paris, France

§Now at: University of Huddersfield, Huddersfield HD1 3DH, UK

¶Deceased

**Now at: University of South Alabama, Mobile, Alabama 36688, USA

††Also at: Università di Sassari, I-07100 Sassari, Italy

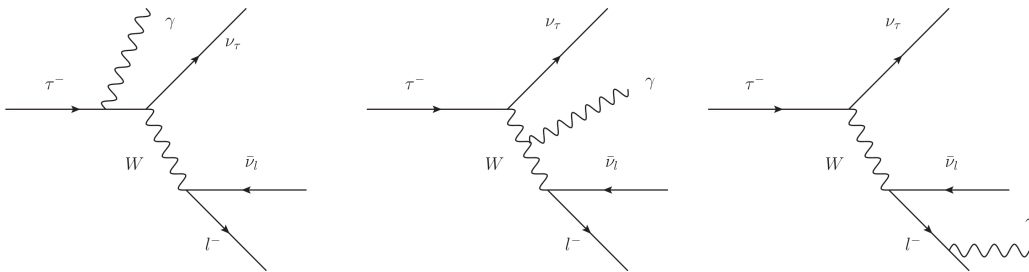


FIG. 1: Standard Model Feynman diagrams for $\tau \rightarrow l\gamma\nu\bar{\nu}$ at tree level.

obtain a τ -pair background sample. Other MC simulated background samples include $\mu^+\mu^-$, $q\bar{q}$ ($u\bar{u}$, $d\bar{d}$, $s\bar{s}$, $c\bar{c}$), and $B\bar{B}$ ($B = B^+$, B^0) events. The $\mu^+\mu^-$ events are generated by KK2f, $q\bar{q}$ events are generated using the JETSET generator [14] while $B\bar{B}$ events are simulated with EVTGEN [15]. The detector response is simulated with GEANT4 [16]. Background from two-photon and Bhabha events is estimated from data.

The signature for $\tau \rightarrow l\gamma\nu\bar{\nu}$ decays is a charged particle (track), identified either as an electron or a muon, and an energy deposit (cluster) in the EMC not associated with any track, the photon. Since τ leptons decay mostly to a single charged particle, events with two well-reconstructed tracks and zero total charge are selected, where no track pair is consistent with being a photon conversion in the detector material. The transverse momentum of each track is required to be $p_T > 0.3$ GeV/ c , the cosine of the polar angle is required to be between -0.75 and 0.95 within the calorimeter acceptance range to ensure good particle identification. The total missing transverse moment of the event is required to be $p_{T,\text{miss}} > 0.5$ GeV/ c . All clusters in the EMC with no associated tracks (neutral clusters) are required to have a minimum energy of 50 MeV. We also reject events with neutral clusters having $E < 110$ MeV if they are within 25 cm of a track, where the distance is measured on the inner wall of the EMC.

Each event is divided into hemispheres (signal and tag hemispheres) in the CM frame by a plane perpendicular to the thrust axis, calculated using all reconstructed charged and neutral particles [17]. For every event, the magnitude of the thrust is required to be between 0.9 and 0.995. The lower limit on the thrust magnitude rejects most $q\bar{q}$ events while the upper limit removes $e^+e^- \rightarrow \mu^+\mu^-$ and Bhabha events. The signal hemisphere must contain one track and one neutral cluster. The tag hemisphere must contain one track, identified either as an electron, muon or pion, and possibly one additional neutral cluster or $n\pi^0$ ($n = 1, 2$). Each π^0 candidate is built up from a pair of neutral clusters with a di-photon invariant mass in the range [100, 160] MeV. To further suppress di-muon and Bhabha events, we reject events where the leptons in the signal and tag hemispheres have the same flavor. Since there are at least three undetected neutrinos in the final state we require

the total energy to be less than 9 GeV. In the signal hemisphere, we require that the distance ($d_{l\gamma}$) between the track and the neutral cluster, measured on the inner wall of the EMC, to be less than 100 cm.

Electrons are identified by applying an Error Correcting Output Code (ECOC) [18] algorithm based on Bagged Decision Tree (BDT) [19] classifiers using as input the ratio of the energy in the EMC to the magnitude of the momentum of the track (E/p), the ionization loss in the tracking system (dE/dx), and the shape of the shower in the electromagnetic calorimeter.

Muon identification makes use of a BDT algorithm, using as input the number of hits in the IFR, the number of interaction lengths traversed, and the energy deposition in the calorimeter. Since muons with momenta less than 500 MeV/ c do not penetrate into the IFR, the BDT also uses information the energy loss dE/dx in the tracking system to maintain a very low $\pi - \mu$ misidentification probability with high selection efficiencies. The electron and muon identification efficiencies are 91% and 62%, respectively. The probability for a π to be misidentified as an e is below 0.1%, while the probability to be misidentified as a μ is around 1% depending on momentum.

After the preselection, both samples are dominated by background events. For the $\tau \rightarrow \mu\gamma\nu\bar{\nu}$ sample, the main background sources are initial-state radiation (ISR), $\tau \rightarrow \pi\pi^0\nu$ decays, $e^+e^- \rightarrow \mu^+\mu^-$ events, and $\tau \rightarrow \pi\nu$ decays. For the $\tau \rightarrow e\gamma\nu\bar{\nu}$ sample, almost all background contribution is from $\tau \rightarrow e\nu\bar{\nu}$ decays in which the electron radiates a photon in the magnetic field of the detector (bremsstrahlung). Further background suppression is obtained by placing requirements on the angle between the lepton and photon in the CM frame ($\cos\theta_{l\gamma}$). For $\tau \rightarrow \mu\gamma\nu\bar{\nu}$ we require $\cos\theta_{l\gamma} > 0.99$, while for $\tau \rightarrow e\gamma\nu\bar{\nu}$ we require $\cos\theta_{l\gamma} > 0.97$ (see Figs. 2 and 3). To reject background from $\tau \rightarrow e\nu\bar{\nu}$ decays in the $\tau \rightarrow e\gamma\nu\bar{\nu}$ sample, we further impose a minimum value for the invariant mass of the lepton-photon pair $M_{l\gamma} \geq 0.14$ GeV/ c^2 for this channel. In addition to the aforementioned quantities, the selection criteria use the energy of the photon and $d_{l\gamma}$. The selection criteria are optimized in order to give the smallest statistical and systematic uncertainty on the branching fractions.

After optimization, for $\tau \rightarrow \mu\gamma\nu\bar{\nu}$, we require $\cos\theta_{l\gamma} \geq 0.99$, $0.10 \leq E_\gamma \leq 2.5$ GeV, $6 \leq d_{l\gamma} \leq 30$ cm, and

$M_{l\gamma} \leq 0.25 \text{ GeV}/c^2$. The requirement on $M_{l\gamma}$ rejects backgrounds from non-signal τ decays. For the $\tau \rightarrow e\gamma\nu\bar{\nu}$ channel, we require $\cos\theta_{l\gamma} \geq 0.97$, $0.22 \leq E_\gamma \leq 2.0 \text{ GeV}$, $8 \leq d_{l\gamma} \leq 65 \text{ cm}$ in addition to $M_{l\gamma} \geq 0.14 \text{ GeV}/c^2$.

The signal efficiencies, the fraction of background events, and the number of events selected in the data are given in Table I.

TABLE I: Signal efficiencies ϵ (%), expected fractional background contribution $f_{\text{bkg}} = N_{\text{bkg}}/(N_{\text{sig}} + N_{\text{bkg}})$, where N_{sig} is the number of signal events and N_{bkg} is the number of background events, and number of observed events (N_{obs}) for the two decay modes after applying all selection criteria. All quoted uncertainties are statistical.

	$\tau \rightarrow \mu\gamma\nu\bar{\nu}$	$\tau \rightarrow e\gamma\nu\bar{\nu}$
ϵ	0.480 ± 0.010	0.105 ± 0.003
f_{bkg}	0.102 ± 0.002	0.156 ± 0.003
N_{obs}	15688 ± 125	18149 ± 135

The branching fraction is determined using

$$\mathcal{B}_l = \frac{N_{\text{obs}}(1 - f_{\text{bkg}})}{2 \sigma_{\tau\tau} \mathcal{L} \epsilon}$$

where N_{obs} is the number of observed events, $\sigma_{\tau\tau}$ is the cross section for τ pair production, \mathcal{L} is the total integrated luminosity, and the signal efficiency ϵ is determined from the MC sample.

After applying all selection criteria, we find

$$\begin{aligned} \mathcal{B}(\tau \rightarrow \mu\gamma\nu\bar{\nu}) &= (3.69 \pm 0.03 \pm 0.10) \times 10^{-3} \\ \mathcal{B}(\tau \rightarrow e\gamma\nu\bar{\nu}) &= (1.847 \pm 0.015 \pm 0.052) \times 10^{-2} \end{aligned}$$

where the first error is statistical and the second is systematic. The systematic uncertainties on signal efficiency and on the number of the expected background events affect the final result, and are summarized in Table II. The most important contributions to the total uncertainty are from the uncertainties on particle identification, and photon detection efficiency.

To estimate the uncertainty on photon detection efficiency, we rely on $e^+e^- \rightarrow \mu^+\mu^-\gamma$ events for the high energy region ($E_\gamma > 1 \text{ GeV}$), and photons from π^0 decays for the low energy region ($E_\gamma < 1 \text{ GeV}$). Using fully reconstructed $e^+e^- \rightarrow \mu^+\mu^-\gamma$ events, we find that the photon detection efficiency for data and MC samples are consistent within 1% for $E_\gamma > 1 \text{ GeV}$. For photon energies $E_\gamma < 1 \text{ GeV}$, we measure the ratio of the branching fractions for $\tau \rightarrow \pi\nu$ and $\tau \rightarrow \rho\nu$ decays. The resulting uncertainty on the π^0 reconstruction efficiency is found to be below 3%. Taking into account the 1.1% uncertainty on the branching fractions, the resulting energy-averaged uncertainty on the single photon detection efficiency is 1.8%. We use this value as the systematic uncertainty in the efficiency for $\tau \rightarrow l\gamma\nu\bar{\nu}$.

The uncertainties on particle identification efficiency are estimated using control samples, by measuring the

deviation of the data and MC efficiencies for tracks with the same kinematic properties. The uncertainty on the efficiency of the electron identification is evaluated using a control sample consisting of radiative and non-radiative Bhabha events, while the uncertainty for muons is an $e^+e^- \rightarrow \mu^+\mu^-\gamma$ control sample. The uncertainty on the probability of misidentifying the pion as a muon or electron is evaluated using samples of $\tau \rightarrow \pi\pi\pi\nu$ decays. The corresponding systematic uncertainty on the efficiency for $\tau \rightarrow l\gamma\nu\bar{\nu}$ is 1.5% for both channels.

For the background estimation, we define control regions that are enhanced with background events. For $\tau \rightarrow \mu\gamma\nu\bar{\nu}$, where the major background contribution is not peaking in $\cos\theta_{\mu\gamma}$, we invert the cut on $\cos\theta_{\mu\gamma}$. For $\cos\theta_{\mu\gamma} < 0.8$, the maximum expected signal rate is 3% of the corresponding background rate. The maximum discrepancy between the MC sample prediction and the number of observed events is 8%, with an excess of events in the MC sample. We take this discrepancy as estimate of the uncertainty on the background prediction. For $\tau \rightarrow e\gamma\nu\bar{\nu}$, where the major background contributions have similar $\cos\theta_{e\gamma}$ distributions as signal, we apply a similar strategy after requiring the invariant mass $M_{l\gamma} < 0.14 \text{ GeV}/c^2$; in this case we take $\cos\theta_{e\gamma} < 0.90$. The maximum contamination of signal events in this region is 10%, and the maximum discrepancy between the prediction and the number of observed events is 4% with an excess of data events. We take this value as an estimate of the uncertainty on the background rate. The errors on the branching fractions due to the uncertainty on background estimates are 0.9% for $\tau \rightarrow \mu\gamma\nu\bar{\nu}$, and 0.7% for $\tau \rightarrow e\gamma\nu\bar{\nu}$, respectively (Table II). Cross-checks of the background estimation are performed by considering the number of events expected and observed in different sideband regions immediately neighboring the signal region for each decay mode and found to be compatible with the aforementioned systematic uncertainties.

All other sources of uncertainty, including current knowledge of the τ branching fractions [13] (BF), total number of τ pairs, limited MC statistics, dependence on selection criteria, and track momentum resolution are found to be smaller than 1.0%.

In conclusion, we have made a measurement of the branching fractions of the radiative leptonic τ decays $\tau \rightarrow e\gamma\nu\bar{\nu}$ and $\tau \rightarrow \mu\gamma\nu\bar{\nu}$, for a minimum photon energy of 10 MeV in the τ rest frame, using the full dataset of e^+e^- collisions collected by *BABAR* at the center-of-mass energy of the $\Upsilon(4S)$ resonance. We find $\mathcal{B}(\tau \rightarrow \mu\gamma\nu\bar{\nu}) = (3.69 \pm 0.03 \pm 0.10) \times 10^{-3}$, and $\mathcal{B}(\tau \rightarrow e\gamma\nu\bar{\nu}) = (1.847 \pm 0.015 \pm 0.052) \times 10^{-2}$, where the first error is statistical and the second is systematic. These results are more precise by a factor of three compared to previous experimental measurements. Our results are in agreement with the Standard Model values at tree level, $\mathcal{B}(\tau \rightarrow \mu\gamma\nu\bar{\nu}) = 3.67 \times 10^{-3}$, and $\mathcal{B}(\tau \rightarrow e\gamma\nu\bar{\nu}) = 1.84 \times 10^{-2}$ [3], and with current experimental bounds.

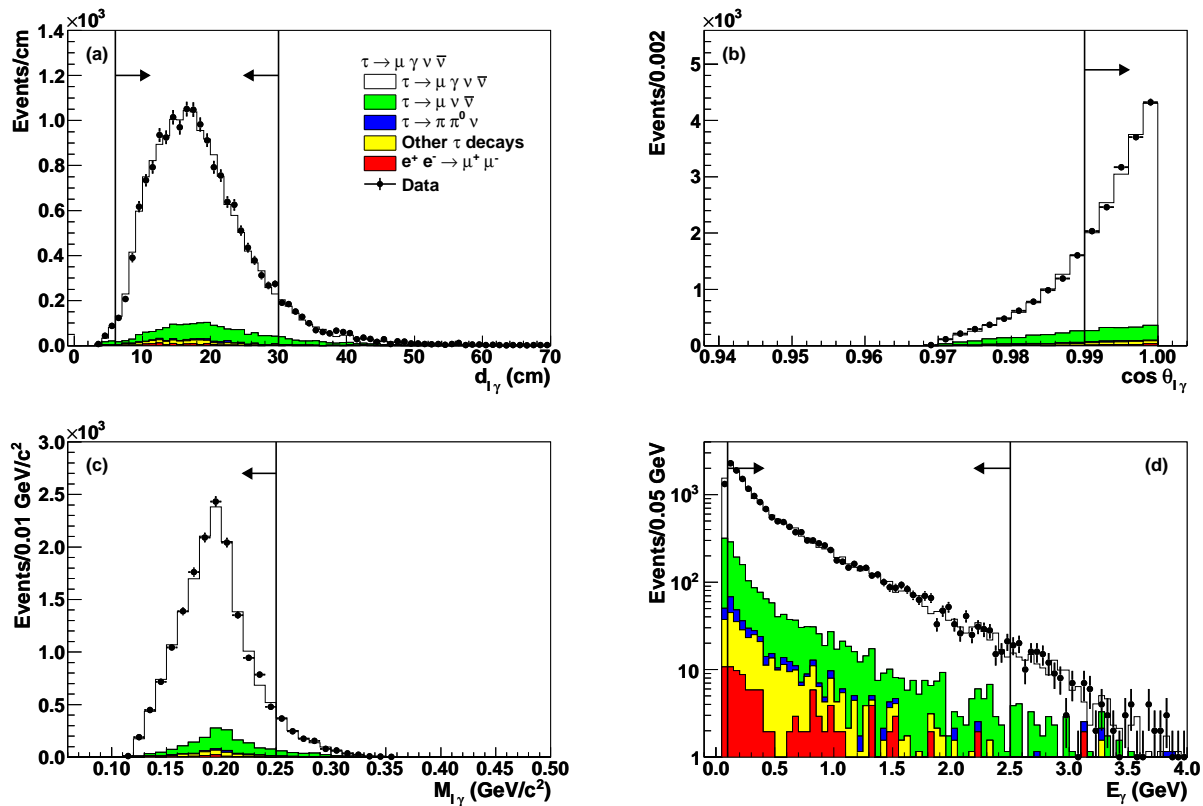


FIG. 2: Selection of the $\tau \rightarrow \mu\gamma\nu\bar{\nu}$: (a) distance between lepton and photon candidates on the inner EMC wall, (b) cosine of the angle between momenta of the lepton and photon candidates in the CM frame, (c) invariant mass of the lepton photon pair, and (d) photon candidate energy in the CM frame for radiative τ decay into a muon after applying all selection criteria except the one on the plotted quantities. The selection criteria on the plotted quantities are highlighted by the vertical lines; we retain the regions indicated by the horizontal arrows.

We are grateful for the extraordinary contributions of our PEP-II colleagues in achieving the excellent luminosity and machine conditions that have made this work possible. The success of this project also relies critically on the expertise and dedication of the computing organizations that support *BABAR*. The collaborating institutions wish to thank SLAC for its support and the kind hospitality extended to them. This work is supported by the US Department of Energy and National Science Foundation, the Natural Sciences and Engineering Research Council (Canada), the Commissariat à l’Energie Atomique and Institut National de Physique Nucléaire et de Physique des Particules (France), the Bundesministerium für Bildung und Forschung and Deutsche Forschungsgemeinschaft (Germany), the Istituto Nazionale di Fisica Nucleare (Italy), the Foundation for Fundamental Research on Matter (The Netherlands), the Research Council of Norway, the Ministry of Education and Science of the Russian Federation, Ministerio de Economía y Competitividad (Spain), the Science and Technology Facilities Council (United Kingdom), and the Binational Science Foundation (U.S.-Israel). Individuals have received support from the Marie-Curie IEF program (European

Union) and the A. P. Sloan Foundation (USA).

TABLE II: Summary of systematic contributions (%) to the branching fraction from the different uncertainty sources for the two signal channels. The total systematic uncertainties are obtained summing in quadrature the various systematic uncertainties for each decay channel.

	$\tau \rightarrow \mu\gamma\nu\bar{\nu}$	$\tau \rightarrow e\gamma\nu\bar{\nu}$
Photon efficiency	1.8	1.8
Particle identification	1.5	1.5
Background evaluation	0.9	0.7
BF [13]	0.7	0.7
Luminosity and cross section	0.6	0.6
MC statistics	0.5	0.6
Selection criteria	0.5	0.5
Trigger selection	0.5	0.6
Track reconstruction	0.3	0.3
Total	2.8	2.8

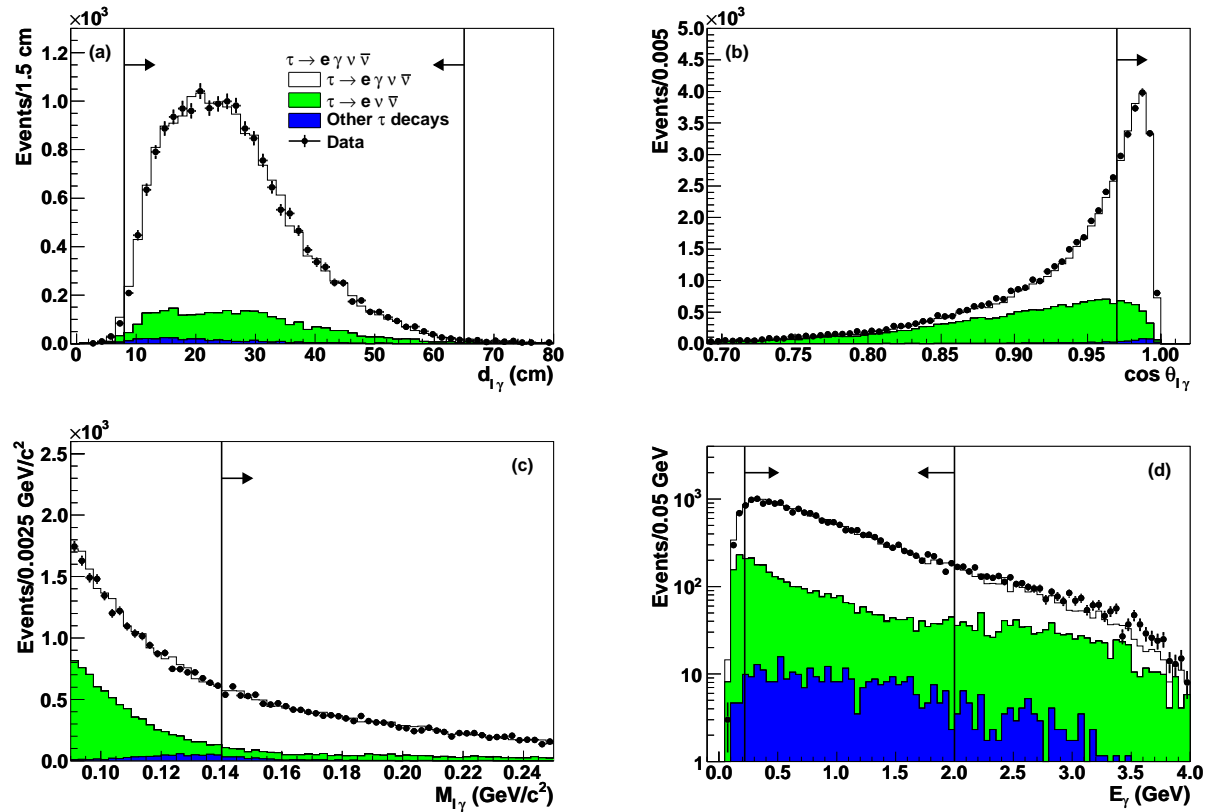


FIG. 3: Selection of the $\tau \rightarrow e\gamma\nu\bar{\nu}$ sample: (a) distance between lepton and photon candidates on the inner EMC wall, (b) cosine of the angle between momenta of the lepton and photon candidates in the CM frame, (c) invariant mass of the lepton photon pair, and (d) photon candidate energy in the CM frame for radiative τ decay into an electron after applying all selection criteria except the one on the plotted quantities. The selection criteria on the plotted quantities are highlighted by the vertical lines; we retain the regions indicated by the horizontal arrows.

-
- [1] L. Michel, Proc. Roy. Soc. Lond. A **63**, 514 (1950).
[2] M. L. Laursen, M. A. Samuel, and A. Sen, Phys. Rev. D **29**, 2652 (1984).
[3] M. Fael, L. Mercolli, and M. Passera, Phys. Rev. D **88**, 093011 (2013).
[4] T. Bergfeld *et al.* (CLEO collaboration), Phys. Rev. Lett. **84**, 830 (2000).
[5] G. Alexander *et al.* (OPAL collaboration), Phys. Lett. B **388**, 437 (1996).
[6] J.P. Lees *et al.* (BABAR Collaboration), Nucl. Instrum. and Methods A **726**, 203 (2013).
[7] S. Banerjee *et al.*, Phys. Rev. D **77**, 054012 (2008).
[8] B. Aubert *et al.* (BABAR collaboration), Nucl. Instrum. Methods Phys. Res., Sect. A **479**, 1 (2002).
[9] B. Aubert *et al.* (BABAR collaboration), Nucl. Instrum. Methods Phys. Res., Sect. A **729**, 615 (2013).
[10] S. Jadach, B. F. Ward, and Z. Was, Comput. Phys. Commun. **130**, 260 (2000).
[11] S. Jadach *et al.*, Comput. Phys. Commun. **76**, 361 (1993).
[12] E. Barberio and Z. Was, Comput. Phys. Commun. **79**, 291 (1994).
[13] K.A. Olive *et al.* (Particle Data Group), Chin. Phys. C **38**, 090001 (2014).
[14] T. Sjostrand, S. Mrenna, and P. Skands, JHEP, **0605**, 026 (2006).
[15] D.J. Lange, Nucl. Instrum. Methods Phys. Res., Sect. A **462**, 152 (2001).
[16] S. Agostinelli *et al.*, Nucl. Instrum. Methods Phys. Res., Sect. A **506**, 250 (2003).
[17] E. Farhi, Phys. Rev. Lett. **39**, 1587 (1977).
[18] T. G. Dietterich and G. Bakiri, J. of Art. Int. Res. **2**, 263 (1995).
[19] E. L. Allwein, R. E. Schapire, and Y. Singer, J. Machine Learning Res. **1**, 113 (2000).